Proceedings of the 8th World Congress on Civil, Structural, and Environmental Engineering (CSEE'23)
Lisbon, Portugal – March 29 – 31, 2023
Paper No. ICGRE 114
DOI: 10.11159/icgre23.114

Hydro-Mechanical Behaviour and Critical State Conditions of Unsaturated Silty Tailings

Gianluca Bella[1] and Guido Musso[2]
[1] Pini Group Ltd
Via Besso 7, Lugano, Switzerland
[2] Politecnico di Torino
Corso Duca degli Abruzzi 24, Torino, Italy
gianluca.bella@pini.group, guido.musso@polito.it

Abstract - The in-depth knowledge of the hydro-mechanical response of tailings finds its practical application as a fundamental tool to reliably assess the stability of the tailing storage facilities, which the high rate of recent collapses poses unacceptable fatalities with environmental and economic damages. This research investigates the hydro-mechanical behaviour of unsaturated fluorite ore tailings collected after the collapse of the Stava dams (Italy). The coupled hydro-mechanical response was studied by carrying out suction-controlled triaxial tests, the Critical State in unsaturated conditions was investigated by imposing different stress-paths, and the experimental results are compared with those obtained on the same material in saturated conditions. Outcomes are interpreted based on the Water Retention Curve (WRC), obtained by performing water retention tests on the same material.

Keywords: tailing dams; Stava; triaxial tests; unsaturated soils; Critical State; Water Retention Curve.

1. Introduction

Tailings dams are geotechnical structures aimed to store wastes resulting from mining processes. Their interactions with the atmosphere result in changes in the level of the water table within the basin, and thus changes in the extent of the unsaturated zone. An experimental characterization of the hydro-mechanical behaviour of tailings under unsaturated conditions is therefore a key tool to assess reliable stability analyses of tailing dams ([1]-[2]). This study presents the main results of an experimental testing campaign carried out on silty tailings. Suction-controlled triaxial tests allowed to investigate the effects of the net stress on the hydro-mechanical behaviour, and results were preliminary interpreted also accounting for the outcomes derived from water retention tests carried out on the same soil. The occurrence of the Critical State in unsaturated conditions was also studied by applying different stress paths.

2. Testing material and experimental apparatus

Tailings used in the current research carried out at Politecnico di Torino (Italy), consist of the silt fraction passing through a sieve n°200, and represent the soil fraction deposited into Stava basins failed in 1985. Its grain size distribution is given in Fig 1, while liquid limit (w_L=27.4%) and plastic limit (w_P=18.0%) show a medium-low plasticity soil (PI=w_L-w_P =9.4%) with 8% in weight of clay size material ([3]-[4]). The specific gravity G_S=2.828 and permeability k=10^{-7}m/s of the silt fraction allows to define the soil as a medium-low permeable, heavy tailings predominantly made of quartz, with significant amount of calcite and fluorite, as resulted by X-ray diffraction analysis ([5]-[6]).

Triaxial tests have been carried out on cylindrical specimens (38 mm initial diameter, 76 mm initial height) prepared at different water content and void ratio. Specimens were prepared by statically compacting the specimens by gradually applying an axial force: a control axial displacement Wykeham Farrance loading frame was used to compact the sample until the desired volume was reached under controlled water content (oedometric conditions). The initial state of the samples is given in Tab.1, together with the control/measurement suction within the triaxial cell and the drainage conditions imposed during the shearing phase. Each triaxial test (Fig. 2) consisted of three phases: i) suction equalization, ii) isotropic consolidation at constant suction, iii) shearing. In the first phase, the desired suction value was imposed by means of the axis translation technique, or by means of the 'vapour equilibrium technique' ([7]). In some cases, this phase was preceded by an isotropic loading phase at constant water content. The second phase was performed by imposing

different confinement in terms of net pressure (difference between average tension and air pressure) between 100 kPa and 800 kPa. The third phase was performed by increasing the axial load at constant water content (undrained conditions), or at constant suction (drained conditions). In one case, the shearing was preceded by a wetting phase of the sample by increasing the water pressure. Table 2 summarizes the test phases for each sample. At the end of the test, the sample is then extracted, weighed, and dried to assess the water content and degree of saturation. Volume changes of the sample were assessed by taking regular laser scans of the sample profile throughout the duration of the test (Fig.3).

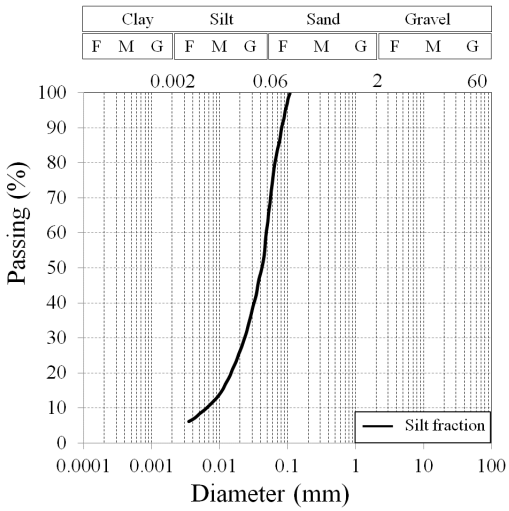

Fig. 1: Grain size distribution of silty Stava tailings.

Table 1. Initial state of Stava samples: dry unit weight (γ_d), void ratio (e_0), water content (w_0), suction control technique (A.T.=axis translation technique, V.E.T.=vapour equilibrium technique), drainage conditions during the shearing phase, and comments (A.=approached; R.=reached; N.R.=not reached).

Sample	γ_d (kN/m^3)	e_0 (-)	w_0 (-)	Suction control technique	Drainage conditions	Critical State
0.70-60-100	16.60	0.70	14.90	A.T.	Undrained	A.
0.70-60-200	16.60	0.70	14.90	A.T.	Undrained	R.
0.70-60-400	16.60	0.70	14.90	A.T.	Undrained	R.
0.60-60-800	17.70	0.60	14.90	A.T.	Undrained	N.R.
0.60-175-200	17.70	0.60	6.40	V.E.T.	Undrained	R.
0.80-90-800	15.70	0.80	5.70	A.T.	Undrained	R.
0.80-90-100	15.70	0.80	14.10	A.T.	Drained (suction imposed)	R.

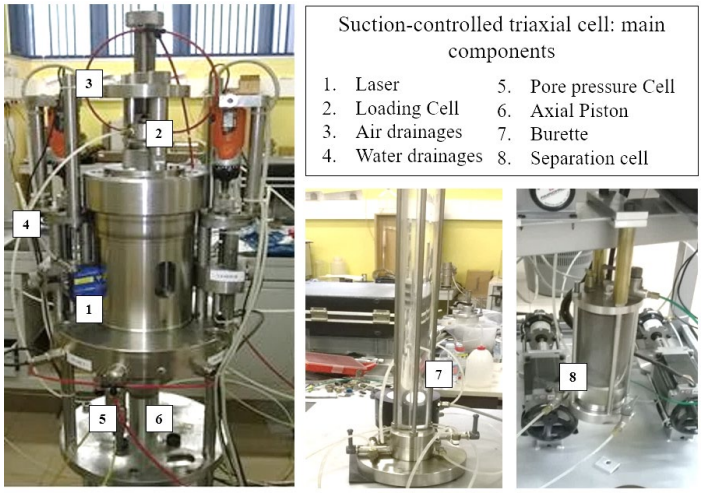

Fig. 2: Suction-controlled triaxial cell: main components.

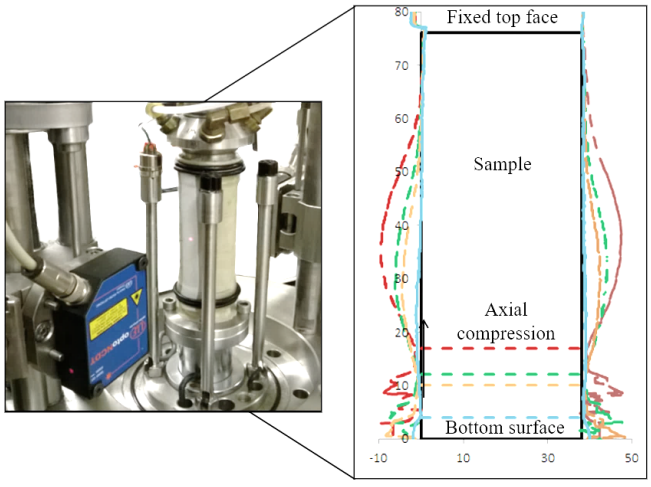

Fig. 3: Typical barrel-shaped deformation given by laser readings at different stages.

.

Table 2. Phases of suction controlled triaxial tests: suction (s), deviatoric stress (q) and net stress (p_{net}). M.=measured, C.=constant.

	Loading w=const	Suction equalization phase			Consolidation phase	Wetting phase			Shearing phase		
Sample	p_{net} (kPa)	s (kPa)	q (kPa)	p_{net} (kPa)	p_{net} (kPa)	s (kPa)	q (kPa)	p_{net} (kPa)	s (kPa)	q (kPa)	p_{net} (kPa)
0.70-60-100	-	s_i→60	0	5-10	5→100	-	-	-	M.	M.	M.
0.70-60-200	-	s_i→60	0	5-10	5→200	-	-	-	M.	M.	M.
0.70-60-400	-	s_i→60	0	5-10	5→400	-	-	-	M.	M.	M.
0.60-60-800	-	s_i→60	0	5-10	5→800	60→20	C.(0)	C.(800)	M.	M.	M.
0.60-175-200	-	s_i→175	0	5-10	5→200	-	-	-	C. (175)	M.	M.
0.80-90-800	100	s_i→90	0	100	5→800	-	-	-	M.	M.	M.
0.80-90-100	100	s_i→90	0	100	-	-	-	-	C. (90)	M.	M.

Outcomes from suction-controlled triaxial tests have been interpreted also accounting for the water retention behaviour of the soil determined by performing water retention tests. The water retention behaviour was investigated on the same material by means of different methods: i) axis translation technique applied into a suction-controlled oedometer (suction range: 0-500 kPa), and vapour equilibrium technique (suction values up to 70 MPa) applied in closed box; ii) total suction measurements with a chilled mirror psychrometer (WP4C) on samples having initial size of 20 mm diameter and height of 10 mm. Details are given in [7].

3. Experimental results

In Section 3.1, the effects of the net stress on the hydro-mechanical response of silty tailing in unsaturated conditions, in terms of suction variations and volume changes are given together a preliminary interpretation based on the WRC obtained from water retention tests. In Section 3.2, the hydro-mechanical behaviour of the unsaturated Stava tailings is studied within the Critical State framework and compared with the response of the same soil under fully saturated conditions.

3.1. Effect of net stress on the hydro-mechanical response in unsaturated conditions

The hydro-mechanical behaviour of unsaturated silt specimens isotropically consolidated at different net stresses is given in Fig. 4. Three specimens 0.70-60-100, 0.70-60-200 and 0.70-60-400 were prepared at the same initial void ratio (e_0=0.70), water content and dry weight. They were equalized at the same suction (s=60 kPa), and then consolidated at different net stresses, respectively p_{net}=100 kPa, p_{net}=200 kPa, and p_{net}=400 kPa. Finally, they were sheared in strain-controlled conditions at constant water content. In all these cases, suction was not changed until the end of consolidation phase. As the shearing phase was performed at constant water content, variations in pore water pressure led to changes in suction. A comparable decrease of suction can be observed for all the three specimens, and such a reduction finds a possible interpretation by considering the evolution of the WRC as described in the following (Fig. 6).

The volume change with the axial strain (solid line) during the undrained shearing phase was estimated based on the laser scanning of the sample profile, as given in Fig. 5. An initial contractive behaviour (volume reduction) is followed by a dilative response (volume increase), by approaching a constant volume condition. However the tendency to dilate reduced with the applied confining stress.

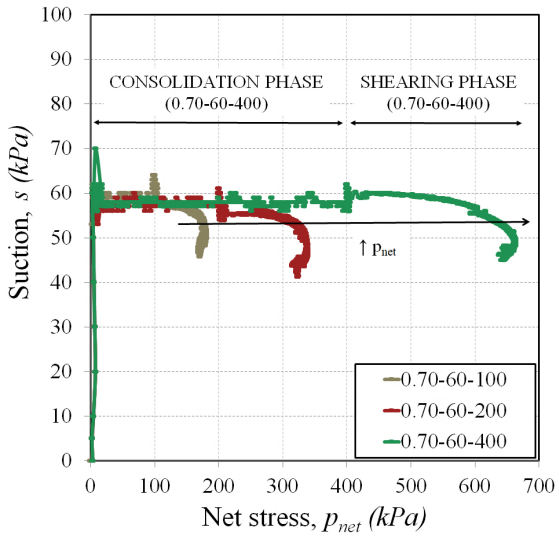

Fig. 4: Evolution of suction for tests 0.70-60-100, 0.70-60-200 and 0.70-60-400.

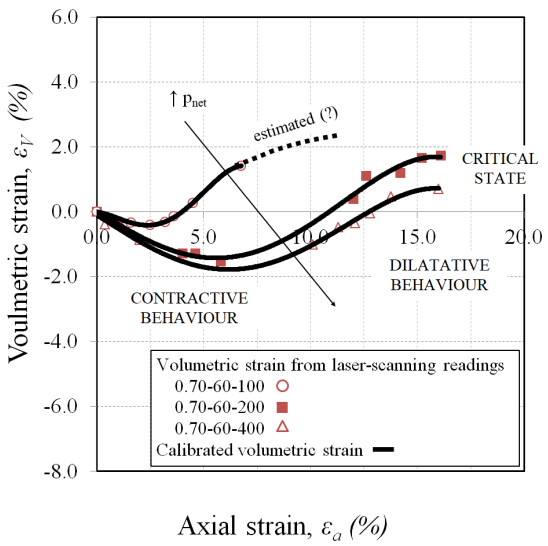

Fig. 5: Volumetric strain with the axial strain during the shearing phase tests 0.70-60-100, 0.70-60-200 and 0.70-60-400.

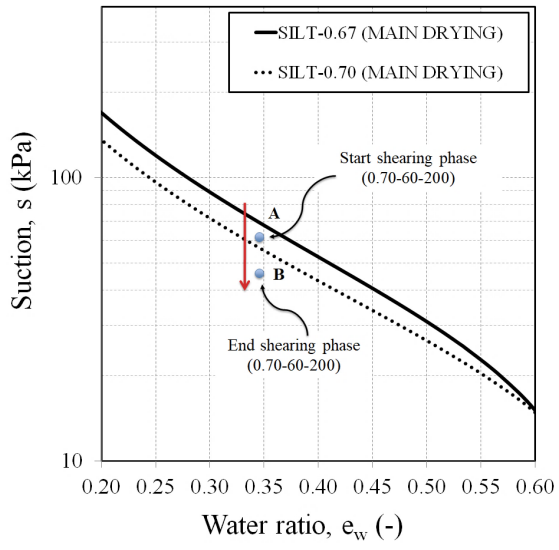

Fig. 6: Hydraulic path of sample 0.70-60-200 and its domain represented by the WRC at section e=0.67 (solid line) and e=0.70 (dotted line).

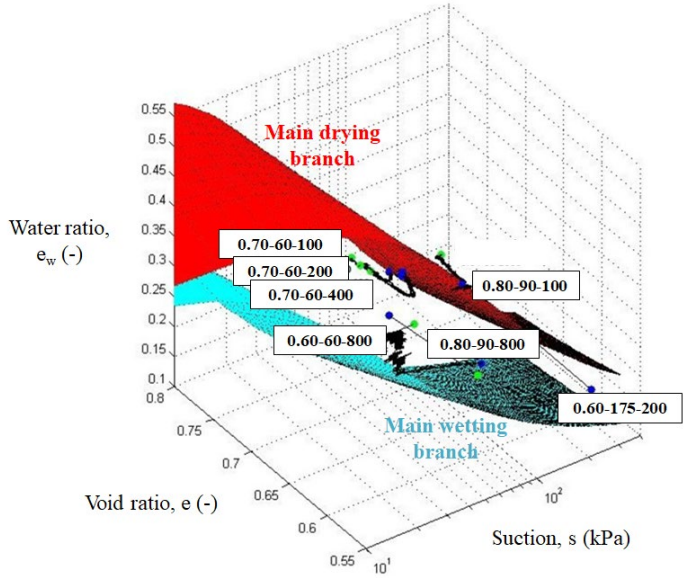

Fig. 7: 3D WRC evaluated from water retention tests, and stress paths obtained from suction-controlled triaxial tests.

A preliminary interpretation of the hydro-mechanical response in terms of suction decrease (Fig. 4) is proposed by estimating the evolution of the water retention curve with void ratio. The WRC is obtained on the same silty tailings by water retention tests, as detailed in [1] and [7]. The model proposed by Gallipoli et al. (2003) was adopted (Eq. (1)), allowing to estimate the evolution of the water retention response with void ratio, and n, m, ψ, Φ parameters are summarized in Tab. 3.

$$Sr = \frac{1}{(1 + [\phi(v-1)^{\psi}s]^{n})^{m}} \quad (1)$$

Table 3 Gallipoli water retention parameters n, m, Φ and ψ for Stava silty samples.

Main drying branch				Main wetting branch			
n (-)	m (-)	Φ (-)	ψ (-)	n (-)	m (-)	Φ (-)	ψ (-)
1.670	0.400	0.281	5.327	1.500	0.330	5.405	7.810

The hydraulic path of specimen 0.70-60-200 is given in Fig. 6 on the (e_w-Sr) plane, where the water ratio e_w is given by knowledge of degree of saturation and void ratio (e_w=Sr·e), while the degree of saturation Sr is defined as the ratio between the water volume and the volume of voids (Sr=V_W/V_V). Points A and B represent the beginning and the end of the shearing phase performed into the suction-controlled triaxial cell. In the same plot, the main drying WRC branches at void ratios equal to those estimated at the beginning (e=0.67) and at the end of the shearing phase (e=0.70), are also given. Since the shearing phase was performed at constant water content, the water ratio (e_w=Sr·e) is constant, so the hydraulic path is basically a vertical line. The initial point A lies close to the main drying branch of WRC(e=0.67), but during the shearing phase, the specimen 0.70-60-200 exhibited a dilative behaviour, so the void ratio increased. A dilative behaviour is associated to changes in the water retention state of the soil toward the drying water retention surface. It could be expected that suction increases due to drying, but suction decreased to approach the main drying branch of the WRC(e=0.70) starting from the WRC(e=0.60) and this is in a good agreement with the experimental data obtained in Fig. 4. The 2D graph given in Fig. 6 represents a cross section at constant void ratio of the WRC surface into the three dimensions space (s-Sr-e) or (s-e-e_w). As given in Fig. 7, all the triaxial stress paths are plotted in the 3D space (s-e-e_w) defined by the water retention surface, that in turn can be assumed as a domain within the stress-paths derived from the suction-controlled triaxial tests could exist.

3.2. Critical State in unsaturated conditions

The Critical State (CS) in saturated conditions is defined as an ultimate condition, attained at large deviator strains. In this state, as deformation proceed with shearing, a saturated volume of soil tends toward an ultimate state in which shearing strains can continue without further variations of volumetric strain, deviatoric stress, or mean effective stresses (Eq. (2)):

$$\frac{\partial \varepsilon_v}{\partial \varepsilon_s} = \frac{\partial q}{\partial \varepsilon_s} = \frac{\partial p'}{\partial \varepsilon_s} = 0 \tag{2}$$

where ε_V is the volumetric strain ($\varepsilon_V=\varepsilon_a+2\varepsilon_r$), ε_s is the deviatoric strain ($\varepsilon_s=2/3[\varepsilon_a-\varepsilon_r]$), q is the deviatoric stress ($q=\sigma_a-\sigma_r$), and p' is the mean effective stress ($p'=1/3[\sigma_a+2\sigma_r]$). If the collection of Critical State conditions attained at different confining pressures is plotted in (q-p') plane, the Critical State condition projects a line known as Critical State Line (CSL) having a constant slope $M=6\cdot\sin(\varphi_{cv})/[3-\sin(\varphi_{cv})]$. In unsaturated conditions no variations of water ratio are expected with shearing strain, so that under such an hypothesis Eq. (2) is modified by adding the ratio $\partial e_w/\partial \varepsilon_s=0$. While the approach to model the Critical State for saturated soils involves three variables (p', q, v) and two critical state equations to predict the deviator stress (q) and the specific volume (v), an extension under unsaturated conditions involves five variables (p, s, q, e, e_w) and three critical state equations to predict the deviator stress, the degree of saturation and the void ratio, when p and s are given ([8], Eq. (3a)-(3c)).

$$f_1(p, s, q, e, e_w) = 0 \tag{3a}$$
$$f_2(p, s, q, e, e_w) = 0 \tag{3b}$$
$$f_3(p, s, q, e, e_w) = 0 \tag{3c}$$

The final states of the suction-controlled triaxial tests are given in Fig. 8. They are represented by squares, triangles, crosses, and circles on the (e_w-p'_B) plane, where p'_B is the mean Bishop effective stress given by knowledge of the net stress p_{net}, suction and degree of saturation ($p'_B = p_{net} + \chi\cdot s$, assuming χ=Sr [9]). The iso-suction curves have been obtained

from the water retention curves on the (s-e_w) plane (Gallipoli model) and represent the suction levels for drying (solid) and wetting (dotted) branches at different Bishop effective stress levels. Each triaxial test is provided with the values of suction s at Critical State or at the end of the test if the critical state was approached or not reached. Despite a certain scattering, it is possible to observe that points related at samples 0.70-60-100, 0.70-60-200, 0.70-60-400, 0.60-60-800, 0.80-90-800 and 0.60-175-200 are quite close to the curve corresponding at the suction value reached at the end of the test.

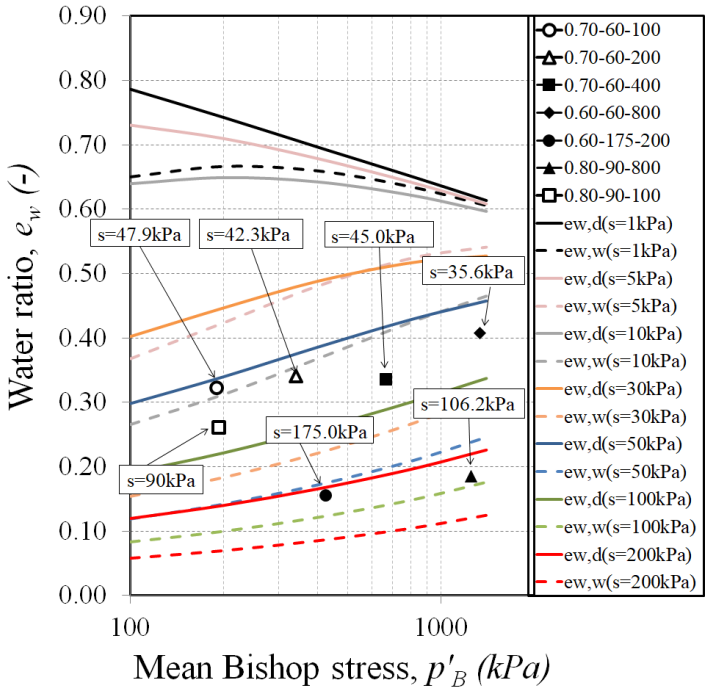

Fig. 8: Points at Critical State in the (e_w-p'$_B$) plane (modified from [7]).

The evolution of the void ratio during the suction-controlled triaxial tests are given in the compression plan in terms of void ratio and mean Bishop stress for unsaturated Stava specimens, as shown in Fig. 9. In the same figure, the final conditions for triaxial tests in saturated conditions ([3]), are given in terms of void ratio e and mean effective stress p'. The empty square points represent the final state of saturated samples: they are connected by a long-dotted line that represents the CSL of Stava silt specimen in saturated conditions. The solid points represent the final state of unsaturated samples. They are connected by a short-dotted line that represents the critical state line of the Stava silt specimen in unsaturated conditions. The two experimental data set, in saturated conditions ([3]) and unsaturated conditions, lie in a narrow area close to a unique critical state line, so the CSL for unsaturated samples is quite close to the CSL for saturated samples, increasing its slope at high stress values. It is worth to note that the Critical State in unsaturated conditions was reached by means of two ways, depending on the initial state (e.g. the initial void ratio) of the sample. Denser specimens approached the CSL by changing their water retention state toward the drying water retention surface as observed for samples 0.70-60-100, 0.70-60-200, 0.70-60-400, 0.60-175-200, and 0.60-60-800. On the other hand, loose samples shown a volume contraction and approached the CSL by changing their water retention state toward the wetting water retention surface, as experience by 0.80-90-800 and 0.80-90-100. The experimental void ratios at Critical State (e_{exp}) were successfully compared with the theoretical void ratio e_{theo} (Fig. 10) predicted by the model proposed by Gallipoli et al. 2003 ([10]-[11]):

$$e_{theo} = [\Gamma - \lambda \cdot \ln(p + s \cdot S_r)] \cdot [1 - a] \cdot \left[1 - e^{(b \cdot \xi)}\right] \quad (4)$$

where Γ and λ are the saturated critical state parameters, a and b are additional parameters to be calibrated in the (e_{cs}/e_{sat}-ξ) plane, and $\xi=f(s)\cdot[1-(e_w/e)]$ is the ratio between the stabilizing force at a given suction and at null suction.

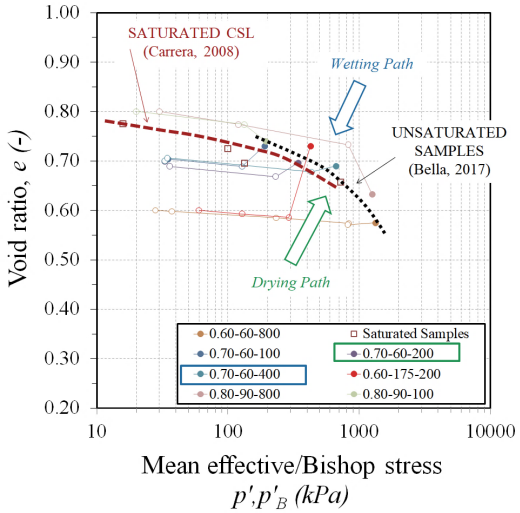

Fig. 9: CSL of saturated silt specimens and evolution of void ratio/Bishop effective stress in unsaturated conditions.

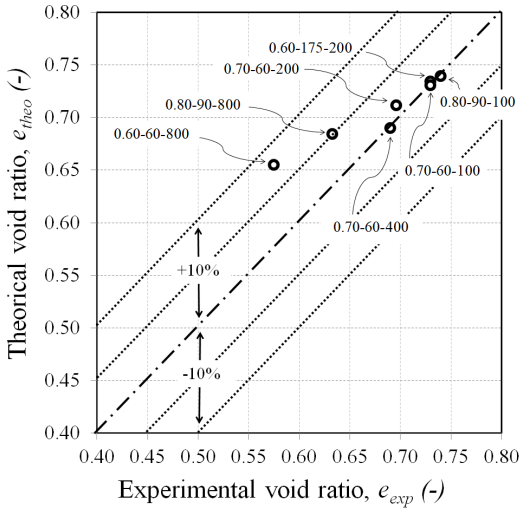

Fig. 10: Experimental void ratio and theorical void ratio as predicted by Gallipoli model.

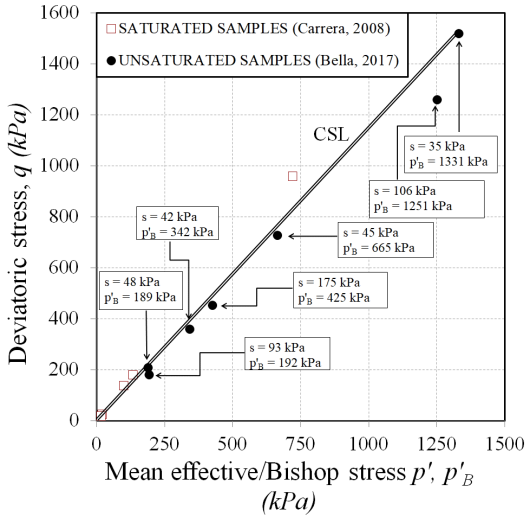

Fig. 11: CSL for saturated silt samples and unsaturated Silty Stava samples.

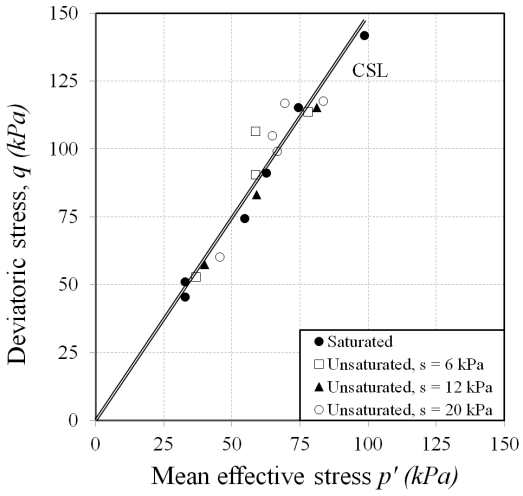

Fig. 12: CSL for saturated silt samples and unsaturated pyroclastic silty-sand (modified from [3]).

If the two set of points at Critical State, respectively unsaturated and saturated results, are plotted together in (q - p'_B/p') plane, again it can be observed that all points are quite aligned, giving a unique critical state line identified by the solid double line (Fig. 11). Similar results were obtained by [12] on normal-consolidated and over-consolidated pyroclastic silty-sand by means of triaxial tests, in saturated and unsaturated conditions (Fig. 12).

4. Conclusion

A detailed understanding of the hydro-mechanical behaviour of tailings in unsaturated conditions is fundamental to approach stability problems of tailing dams. Partially saturated silty tailings were characterized by means of water retention and suction-controlled triaxial tests performed under constant water content, and under constant suction conditions. Due to the coupling of hydraulic and mechanical behaviour in unsaturated conditions, the effect of net stress on the suction and volume changes is investigated and successfully interpreted based on the water retention curves. The Critical State was approached in the compression plane both from drying and wetting side. Outcomes were compared with those obtained in a previous experimental campaign on the same soil in saturated conditions. By adopting a Bishop like effective stress, it was found that the soil strength is characterized by a single Critical State Line, both in saturated and unsaturated conditions.

References

[1] G. Bella, "Water retention behaviour of tailings in unsaturated conditions", *Geomechanics and Engineering, An Int'l Journal*, vol. 26, no. 02, pp. 117-132, 2021.

[2] G. Bella, "Mechanical Response of Tailings Under Monotonic Triaxial Tests in Unsaturated and Nearly Saturated Conditions", *Proceedings of the 8th International Conference on Geotechnical Research and Engineering (ICGRE 2022)*, Online - March, 29-31, 2023.

[3] A. Carrera, "Mechanical behaviour of Stava tailings", *Ph.D. dissertation*, Dept. Struct. Build. and Geotech. Eng., Politecnico di Torino, Italy, 2008.

[4] A. Carrera, M. Coop and R. Lancellotta, "Influence of grading on the mechanical behaviour of Stava tailings", *Géotechnique*, vol. 61, no. 11, pp. 935-946, 2011.

[5] G. Bella, M. Barbero, F. Lameiras, T. Esposito and F. Barpi, "Chemical-Physical Characterization of Stava Tailings Subjected to an Innovative Aging Technique", *Proceedings of the 7th International Conference on Geotechnical Research and Engineering (ICGRE 2022)*, Online - April, 10-12, 2022.

[6] G. Bella, F.S. Lameiras, T. Esposito, M. Barbero and F. Barpi, "Aging Simulation of the Tailings from Stava Fluorite Extraction by Exposure to Gamma Rays", *Revista Escola de Minas*, vol. 70, no. 04, pp. 483-490, 2017.

[7] G. Bella, "Hydro-Mechanical Behaviour of tailings in Unsaturated Conditions", *Ph.D. dissertation*, Dept. Struct. Build. and Geotech. Eng., Politecnico di Torino, Italy, 2017.

[8] A. Tarantino, "A possible critical state framework for unsaturated compacted soils", Technical Note, *Géotechnique*, vol. 57, no. 04, pp. 385-389, 2007.

[9] A. Tarantino and G. El Mountassir, "Making unsaturated soil mechanics accessible for engineers: Preliminary hydraulic–mechanical characterisation and stability assessment", *Engineering Geology*, vol. 165, no. 89, pp. 89-104, 2013.

[10] D. Gallipoli, A. Gens, R. Sharma and J. Vaunat, "An elasto-plastic model for unsaturated soil incorporating the effects of suction and degree of saturation on mechanical behaviour", *Geotechnique*, vol. 53, no. 01, pp. 123-135, 2003.

[11] D. Gallipoli, S.J. Wheeler and M. Karstunen, "Modelling the variation of degree of saturation in a deformable unsaturated soil", *Geotechnique*, vol. 53, no. 01, pp. 105-112, 2003.

[12] M. Nicotera, R. Papa and G. Urciuoli, "The hydro-mechanical behaviour of unsaturated pyroclastic soils: An experimental investigation", *Engineering Geology*, vol. 195, pp. 70-84, 2015.